Physiological restraint of Bak by Bcl-x_L is essential for cell survival

Erinna F. Lee,[1,2,3,4,5] Stephanie Grabow,[1,2] Stephane Chappaz,[1,2] Grant Dewson,[1,2] Colin Hockings,[1,2] Ruth M. Kluck,[1,2] Marlyse A. Debrincat,[1,2] Daniel H. Gray,[1,2] Matthew T. Witkowski,[1,2] Marco Evangelista,[4,5] Anne Pettikiriarachchi,[1] Philippe Bouillet,[1,2] Rachael M. Lane,[1] Peter E. Czabotar,[1,2] Peter M. Colman,[1,2] Brian J. Smith,[3] Benjamin T. Kile,[1,2,6] and W. Douglas Fairlie[1,2,3,4,5,6]

[1]The Walter and Eliza Hall Institute of Medical Research, Parkville, Victoria 3052, Australia; [2]Department of Medical Biology, The University of Melbourne, Parkville, Victoria 3010, Australia; [3]Department of Chemistry and Physics, La Trobe Institute for Molecular Science, La Trobe University, Bundoora, Victoria 3086, Australia; [4]Olivia Newton-John Cancer Research Institute, Heidelberg, Victoria 3084, Australia; [5]School of Cancer Medicine, La Trobe University, Melbourne, Victoria 3084, Australia

Due to the myriad interactions between prosurvival and proapoptotic members of the Bcl-2 family of proteins, establishing the mechanisms that regulate the intrinsic apoptotic pathway has proven challenging. Mechanistic insights have primarily been gleaned from in vitro studies because genetic approaches in mammals that produce unambiguous data are difficult to design. Here we describe a mutation in mouse and human Bak that specifically disrupts its interaction with the prosurvival protein Bcl-x_L. Substitution of Glu75 in mBak (hBAK Q77) for leucine does not affect the three-dimensional structure of Bak or killing activity but reduces its affinity for Bcl-x_L via loss of a single hydrogen bond. Using this mutant, we investigated the requirement for physical restraint of Bak by Bcl-x_L in apoptotic regulation. In vitro, *Bak*^{Q75L} cells were significantly more sensitive to various apoptotic stimuli. In vivo, loss of Bcl-x_L binding to Bak led to significant defects in T-cell and blood platelet survival. Thus, we provide the first definitive in vivo evidence that prosurvival proteins maintain cellular viability by interacting with and inhibiting Bak.

[*Keywords*: apoptosis; Bcl-2; BH3; Bak; Bcl-x_L]

Supplemental material is available for this article.

Received February 11, 2016; revised version accepted April 18, 2016.

The Bcl-2 family of proteins determines cell fate by regulating the integrity of the mitochondrial outer membrane (MOM). It comprises three subgroups. The first includes the prosurvival proteins (Bcl-2, Bcl-x_L, Bcl-w, Mcl-1, and BFL-1/A1), which prevent apoptosis by inhibiting the activation of a second group consisting of Bax and Bak (and possibly Bok). The latter represents the essential mediators of the pathway. Upon activation, they oligomerize and form pore-like structures in the MOM. The third group contains the BH3-only proteins (e.g., Bim, Bid, Puma, and Noxa), which lie upstream and are responsible for the initiation of apoptosis.

Two alternative mechanisms have been proposed for how apoptosis is regulated by prosurvival proteins. One of these ("mode 1") proposes that Bcl-2 and other prosurvival proteins sequester a subset of BH3-only proteins—the so-called "activators" (e.g., Bim and Bid)—that can directly engage and activate Bax and Bak (Cheng et al. 2001; Letai et al. 2002; Kuwana et al. 2005; Llambi et al. 2011). Here, proapoptotic signals lead to displacement of the activators by competitive interactions with "sensitizer" BH3-only proteins (e.g., Bad), thereby allowing Bax/Bak oligomerization and consequent MOM damage. In the second mechanism ("mode 2"), prosurvival proteins physically engage "activated" Bax/Bak to prevent their oligomerization and pore formation (Willis et al. 2005, 2007; Fletcher et al. 2008; Llambi et al. 2011). Apoptosis occurs when BH3-only proteins disrupt this interaction and unleash Bak and Bax. While there was some controversy over which of these mechanisms best describes how apoptosis is regulated, evidence from various experimental approaches suggests that both contribute to apoptotic control (the "unified," "interconnected hierarchical," and "embedded together" models) (Leber et al. 2010; Llambi et al. 2011; Chen et al. 2015).

Although the studies that uncovered these mechanisms provide persuasive insights into how cell death is regulated, they are all essentially based on in vitro evidence, as it has proven very difficult to generate conclusive data in

[6]**These authors contributed equally to this work.**
Corresponding authors: doug.fairlie@onjcri.org.au, kile@wehi.edu.au
Article published online ahead of print. Article and publication date are is online at http://www.genesdev.org/cgi/doi/10.1101/gad.279414.116.

vivo. For example, despite the range of profound cell and organ defects provoked by genetic deletion of one or more prosurvival proteins in mice, it is impossible to distinguish whether these phenotypes reflect a role for mode 1 and/or mode 2 regulation (Youle and Strasser 2008). Nevertheless, studies using BH3-only protein chimeric knock-in or quadruple BH3-only protein knockout mice have provided some evidence for physiological roles of mode 1 regulation and ex vivo evidence for mode 2 (Merino et al. 2009; Chen et al. 2015). Here, we describe the first mouse model to provide evidence for physiological roles for mode 2 regulation in vivo.

Results

Mutations in the BAK BH3 domain that specifically disrupt BCL-X_L binding

In considering the mode 2 mechanism of apoptotic control, we hypothesized that specific mutations could be introduced into Bax or Bak that would disrupt binding to prosurvival Bcl-2 proteins without influencing any potential mode 1 interactions (Fig. 1A). We reasoned that Bak would be more tractable than Bax, as it is regulated by fewer prosurvival proteins and does not require translocation to the MOM to function (Willis et al. 2005, 2007; Fletcher et al. 2008; Llambi et al. 2011). Mode 2 regulation of Bak is mediated by its BH3 domain (Willis et al. 2005; Chen et al. 2015), which is also critical for Bak homodimerization and proapoptotic activity (Dewson et al. 2008). Hence, we set out to identify Bak BH3 domain mutations that influenced interactions with its key prosurvival protein regulators, Mcl-1 and Bcl-x_L (Willis et al. 2005; Chen et al. 2015), but did not influence assembly into the higher-order Bak oligomers required to mediate MOM damage.

First, we performed alanine-scanning mutagenesis of the human BAK BH3 domain as previously described (Lee et al. 2008). As expected, the conserved residues that define BH3 domains (i.e., V74, L78, I81, D83, and I85 and small residues G75 and G82) were most important for prosurvival protein binding. Individual substitution of each to alanine significantly reduced the affinity of hBAK for BCL-X_L and MCL-1 (Fig. 1B–E). Furthermore, these mutants of full-length BAK failed to homodimerize to a significant degree in response to tBID treatment (Fig. 1F) and, consequently, to kill $Bax^{-/-}/Bak^{-/-}$ mouse embryonic fibroblasts (MEFs) reconstituted with them (Fig. 1G). In contrast, the R76A and Q77A mutants, which exhibited a fourfold to eightfold reduction in binding to BCL-X_L (Fig. 1B,D), dimerized more efficiently in response to tBID and killed $Bax^{-/-}/Bak^{-/-}$ MEFs. These data suggest that the hBAK R76A and Q77A mutations specifically disrupt mode 2 interactions with BCL-X_L but do not affect the ability of BAK to homodimerize and mediate cell death.

A mouse model of mode 2 prosurvival function

In parallel with our biochemical studies, we performed an *N*-ethyl-*N*-nitrosourea (ENU) mutagenesis screen in mice and identified a missense point mutation in *Bak* that, remarkably, was predicted to encode a leucine substitution at residue Glu75 (Q75L), equivalent to Q77L in hBAK. We therefore examined whether the mBak Q75L mutation also influenced prosurvival protein binding. An mBak Q75L BH3 synthetic peptide bound mBcl-x_L approximately sevenfold weaker than the wild-type Bak BH3 (Fig. 2A), an effect very similar to that of the hBAK BH3 Q77A mutation (Fig. 1B,D). Binding to Mcl-1, Bcl-w, and A1 was unaffected, while the affinity for Bcl-2 was 2.5-fold weaker than wild-type mBak BH3. Consistent with these data, in coimmunoprecipitation experiments using mouse liver mitochondria (MLM) purified from wild-type, $Bak^{+/Q75L}$, or $Bak^{Q75L/Q75L}$ mice, Mcl-1 associated nearly equally with full-length Bak or Bak^{Q75L} (Fig. 2B). Furthermore, Bcl-x_L coimmunoprecipitated only with wild-type Bak present in $Bak^{+/+}$ and $Bak^{+/Q75L}$ MLM but not with Bak^{Q75L} from the homozygous $Bak^{Q75L/Q75L}$ MLM (Fig. 2B). The Q75L mutation did not affect Bak homodimerization following tBID activation, and its association with VDAC2, a negative regulator of Bak (Cheng et al. 2003; Lazarou et al. 2010), was also unimpaired (Fig. 2C). Hence, the Bak^{Q75L} mouse represents an in vivo reporter for the interaction between Bak and Bcl-x_L.

Structural basis for the reduced affinity of Bak^{Q75L} for BCL-X_L

We next examined the effect of the Bak^{Q75L} mutation on the protein's global structure and interaction with Bcl-x_L. We focused on $hBAK^{Q77L}$ to enable comparison with published hBAK structures. BAK^{Q77L} adopted a three-dimensional structure essentially identical to that of wild-type hBAK (root mean square deviation [RMSD] 0.187 Å), with the L77 side chain positioned similarly to that of the wild-type Q77 residue (Fig. 2D; Supplemental Table S1). Hence, the Q77L mutation does not cause significant structural changes in BAK. We also solved the structures of the wild-type and mutant BAK BH3:BCL-X_L complexes (Supplemental Table S1). Both BH3 domains (human wild-type BAK and mouse mutant Bak) engaged the hydrophobic BH3 domain-binding groove of BCL-X_L in the canonical manner (Fig. 2E). Two residues on BCL-X_L (Y101 and Q111) potentially hydrogen-bond to Q77 in hBAK BH3 (Fig. 2F), and this bond is absent when Q77 is substituted for leucine (Fig. 2G). To determine whether the loss of affinity for BCL-X_L is due to disruption of these interactions, we generated Y101F, Q111A, and Y101F/Q111A mutants of mBcl-x_L. Both the Y101F and the Y101F/Q111A mutants bound to wild-type mBak BH3 ~3.5-fold more weakly than to wild-type BCL-X_L, while the Q111A mutation had no impact (data not shown). Hence, the disruptive effect of the Bak^{Q75L} mutation on binding to Bcl-x_L is likely attributed to the loss of a hydrogen bond between Bak Q75 and Bcl-x_L Y101.

The Bak^{Q75L} mutation renders cells more sensitive to proapoptotic agents

Given that only the Bak:Bcl-x_L interaction was significantly impaired in Bak^{Q75L} mice, they provided an ideal

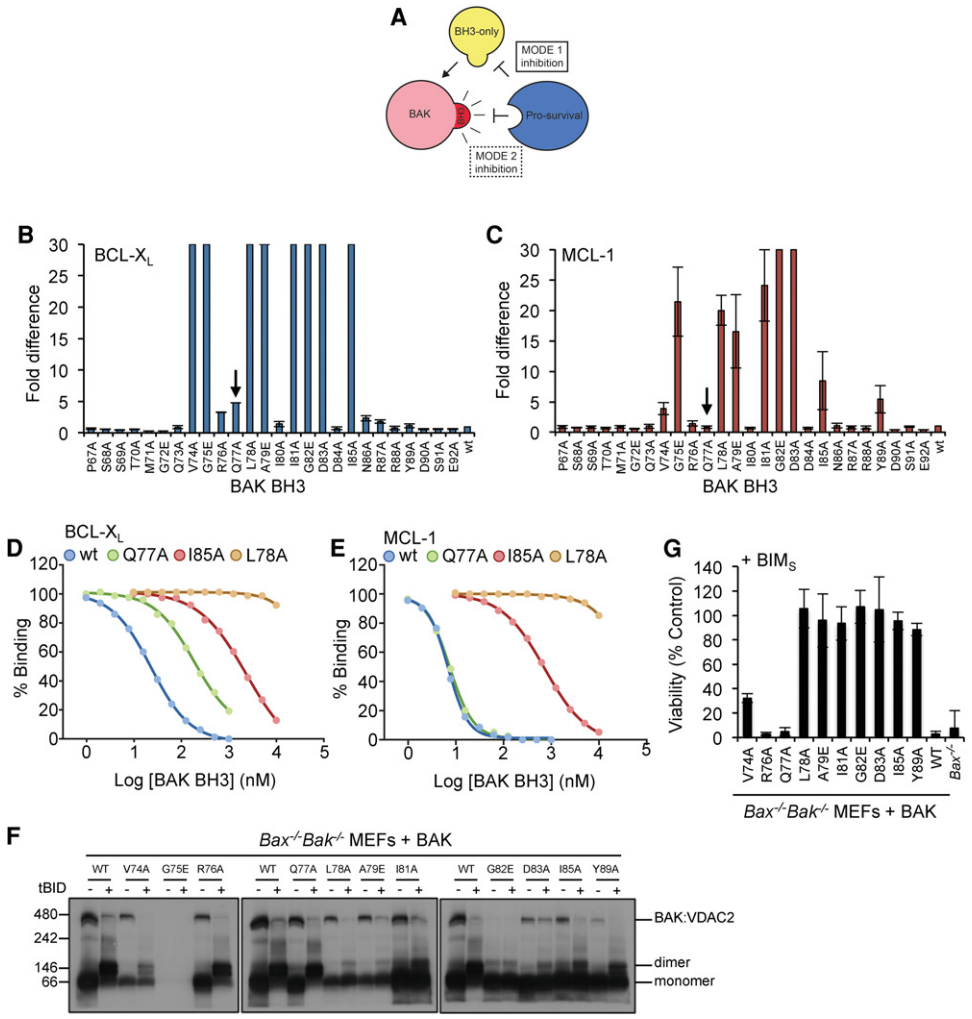

Figure 1. A BAK BH3 mutation that affects BCL-X_L binding but not BAK function. (*A*) Schematic of mode 1 and mode 2 mechanisms of apoptosis regulation. (*B*,*C*) To investigate the contribution of each residue within the BAK BH3 domain for binding either BCL-X_L (*B*) or MCL-1 (*C*), each residue of a phage-displayed BAK BH3 peptide was mutated to alanine (except for native alanines or glycines, which were replaced with glutamic acid), and their relative affinities (IC_{50}) were determined by solution competition ELISA. The data represent the fold-reduction in binding of the mutant sequence compared with wild-type BAK BH3. The upper limit on the *Y*-axes was set to >30-fold reduction based on the IC_{50} (>10 µM) of a nonbinding mutant (G82E) independently confirmed in competition binding assays using surface plasmon resonance. (*D*,*E*) Representative binding curves for wild-type BAK BH3 and mutants in competition binding assays with BCL-x_L (*D*) and MCL-1 (*E*). Mutants such as L78A and I85A show significantly reduced binding to both BCL-x_L (*D*) and MCL-1 (*E*), while BAK Q77A impacts (eightfold reduction) only on BCL-X_L binding. (*F*) BAK BH3 mutations except R76A and Q77A impair the ability of BAK to homodimerize. Permeabilized $Bax^{-/-}/Bak^{-/-}$ mouse embryonic fibroblasts (MEFs) expressing BAK BH3 mutants were treated with tBID, and BAK dimerization was assessed by BN PAGE and Western blotting. Note that BAK G75E did not express at levels detectable by Western blotting. The blot was probed with anti-BAK antibody. (*G*) Mutation of key residues involved in prosurvival protein binding rendered BAK inactive, except R76A and Q77A. $Bax^{-/-}/Bak^{-/-}$ MEFs expressing BAK BH3 mutants were transduced with a retrovirus to express either BIM_S or the inert mutant BIM_S4E, and colony numbers were determined after 7 d. Viability is the number of colonies in the BIM_S-expressing cells relative to those expressing BIM_S4E. Data are presented as mean ± SD of $n = 3$ experiments in *B*, *C*, and *G*.

system to probe the requirement for prosurvival protein inhibition by mode 2 both in vitro and in vivo. We first examined MEFs from Bak^{Q75L} embryos. As wild-type MEFs are dependent on both Mcl-1 and Bcl-x_L for their survival (Willis et al. 2005; Chen et al. 2015), we hypothesized that MEFs derived from Bak^{Q75L} embryos would be primarily dependent on Mcl-1. Consistent with this, $Bak^{+/Q75L}$ and $Bak^{Q75L/Q75L}$ MEFs died following expression of the MCL-1-selective BH3-only protein NOXA, as did $Bcl\text{-}x^{-/-}$ MEFs (Fig. 3A). In contrast, NOXA expression did not affect wild-type MEF survival. We therefore tested other proapoptotic stimuli. Approximately fourfold less of the tBID variant M97A that fails to bind BCL-X_L (Supplemental Fig. S1A) was required to induce cytochrome *c* release in $Bak^{Q75L/Q75L}$ MEFs relative to wild-type cells (1.1 nM vs. 4.5 nM) (Fig. 3B). Accordingly, fourfold more recombinant BCL-X_L (25 nM vs. 6.3 nM) was required to prevent cytochrome *c* release in $Bak^{Q75L/Q75L}$

MEFs compared with wild-type cells following treatment with tBIDM97A (Fig. 3C). Furthermore, $Bak^{+/Q75L}$ and $Bak^{Q75L/Q75}$ MEFs were significantly more sensitive than wild-type cells to drug-induced apoptosis in response to bortezomib, actinomycin D, cycloheximide, and etoposide (Fig. 3D–G). In most cases Bak^{Q75L} MEFs were as sensitive as cells deficient in Bcl-x_L (where inhibition of both mode 1 and mode 2 by Bcl-x_L is absent). Bak levels are essentially the same in all cell lines; hence, this should not have influenced the outcome in these experiments (Supplemental Fig. S1B). These data indicate that the Bak^{Q75L} mutation reduces the capacity of Bcl-x_L to inhibit Bak's killing activity and that the physical interaction between the two proteins significantly influences the response to apoptotic stimuli.

Mode 2 is required for T-cell development

Having established a role for mode 2 regulation of apoptosis in response to exogenous apoptotic stimuli, we next examined the requirement for mode 2 in vivo. Given the critical importance of Bcl-x_L in thymic T-cell development (Ma et al. 1995; Motoyama et al. 1995), we analyzed thymi of Bak^{Q75L} mutants. All major T-cell subtypes were reduced by approximately threefold to fourfold in $Bak^{Q75L/Q75L}$ mice relative to wild-type mice, although the loss of $CD4^+CD8^+$ double-positive thymocytes accounted for most of this reduction (Fig. 4A). Upon competitive bone marrow transplantation, the representation of $Bak^{Q75L/Q75L}$ cells was normal in hematopoietic progenitor cells (Fig. 4B), whereas it was decreased in thymocytes from the double-negative stage onwards (Fig. 4C). The representation of mutant cells was not further decreased within the splenic naïve T-cell compartments (Fig. 4D), altogether suggesting that the Bak^{Q75L} mutation specifically compromises competitiveness in developing thymocytes. Hence, the reduced thymic cellularity in Bak^{Q75L}

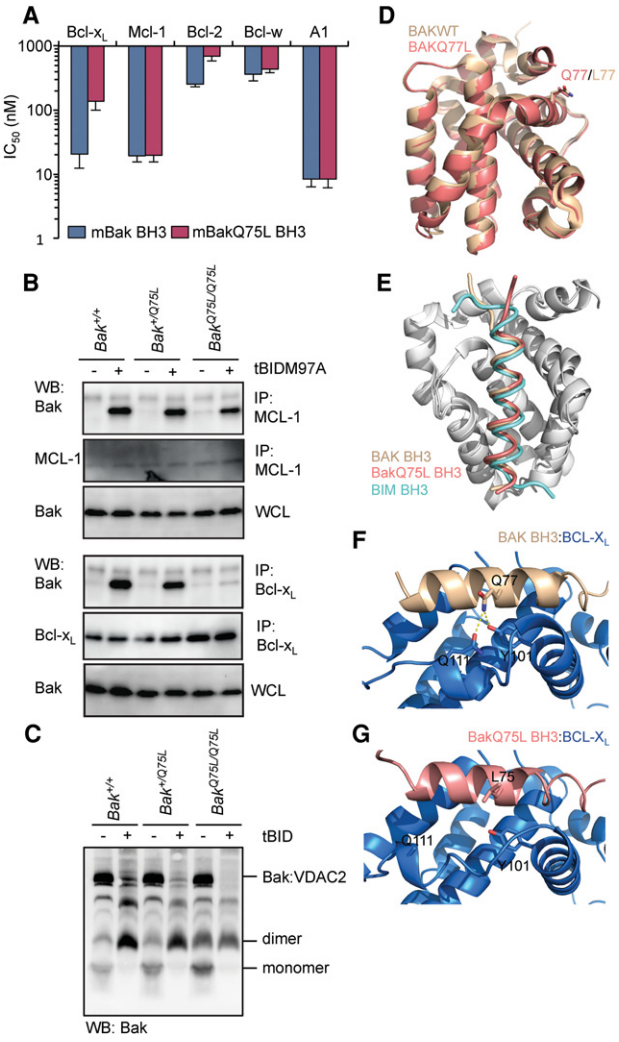

Figure 2. The BakQ75L mutation impairs heterodimerization with Bcl-x_L. (*A*) Relative binding affinities of wild-type Bak BH3 or BakQ75L BH3 peptides for prosurvival proteins determined by competitive surface plasmon resonance binding assays. The Q75L mutation had the most significant effect on Bcl-x_L binding, similar to the equivalent mutation in hBAK BH3. Data are presented as mean ± SD of $n = 3$ experiments. (*B*) The effect of the Q75L mutation in full-length Bak on Bcl-x_L and Mcl-1 binding was assessed by coimmunoprecipitation. Following treatment of MLM from wild-type, $Bak^{+/Q75L}$, and $Bak^{Q75L/Q75L}$ mice with tBIDM97A, Mcl-1 coimmunoprecipitated with Bak from all mitochondria. In contrast, only Bak from $Bak^{+/+}$ or $Bak^{+/Q75L}$ mitochondria, but not from $Bak^{Q75L/Q75L}$ mitochondria, bound to BCL-X_L. tBIDM97A is a mutant of tBID that retains the ability to activate Bax and Bak but has a greatly reduced capacity to engage prosurvival proteins compared with wild-type tBID (Supplemental Fig. S1A), thereby eliminating any potential complications that arise in these types of experiments when the BH3-only activator can also inhibit the prosurvival protein:Bak interaction being examined. (IP) Immunoprecipitation; (WCL) whole-cell lysate; (WB) Western blot. (*C*) The Q75L substitution did not affect Bak homodimerization or association with VDAC2. Permeabilized MEFs from $Bak^{+/+}$, $Bak^{+/Q75L}$, and $Bak^{Q75L/Q75L}$ embryos were untreated (–) or treated with tBID (+), and lysates were analyzed by Blue Native PAGE. (*D*) The X-ray crystal structure of hBAK (without its C-terminal hydrophobic tail) with the mutation (Q77L; Protein Data Bank [PDB] ID 5FMI) equivalent to the Q75L mutation in mBak overlayed with a previously published structure of hBAK (PDB ID 2IMS). The overall structure of BAKQ77L was not significantly affected by the mutation, and the side chain of L77 is oriented identically to the wild-type glutamine at this position on the solvent-exposed surface of the α2 (BH3) helix. Human BAK is 78% identical to mBak, and the Q77L mutation had an identical effect on hBAK BH3 binding to hBCL-X_L. (*E*) Overlay of the crystal structures of hBCL-X_L bound (shown in gray) to wild-type hBAK BH3 (PDB ID 5FMK), mBakQ75L (PDB ID 5FMJ), or BIM BH3 (PDB ID 3FDL) (Lee et al. 2009) peptides. All peptides bind similarly in the canonical BH3 ligand-binding groove. (*F*) In the wild-type hBAK BH3: hBCL-X_L complex, Q77 can potentially hydrogen-bond with Y101 and/or Q111 on BCL-X_L. (*G*) The crystal structure of BCL-X_L complexed with mBakBH3 Q75L, showing that this hydrogen bond network is lost when Q75 is replaced with leucine, explaining the reduced affinity for Bcl-x_L. No electron density was apparent for the side chain of Q111 in this complex structure.

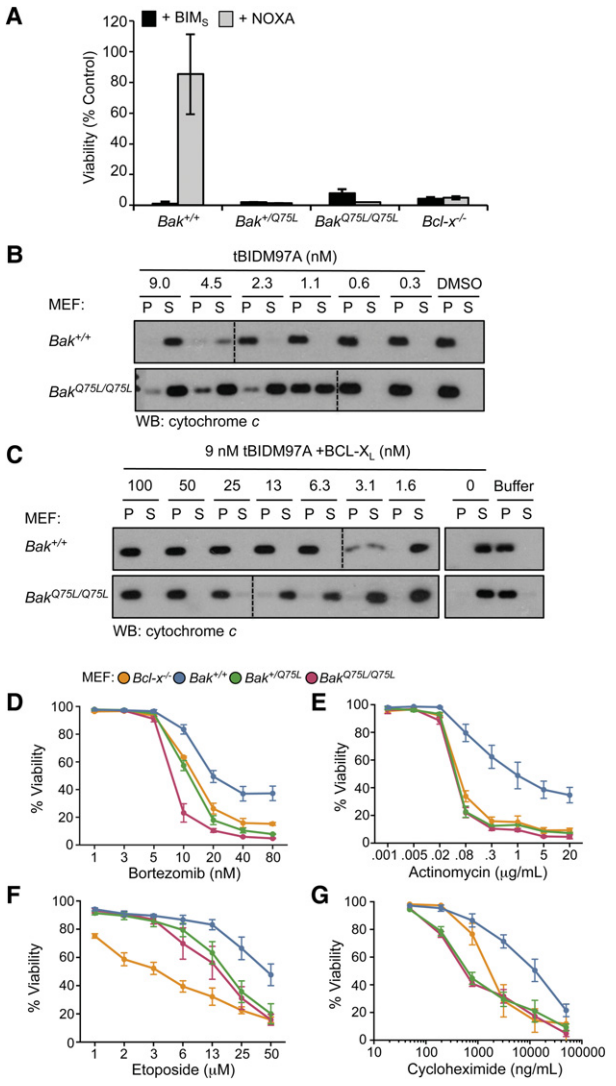

Figure 3. The Bak Q75L mutation renders cells more sensitive to apoptotic stimuli. (*A*) The killing activity of BH3-only proteins BIM_S (promiscuous prosurvival protein binder) and NOXA (MCL-1-selective) expressed retrovirally in MEFs. The Bak Q75L renders MEFs sensitive to Mcl-1 antagonism. (*B*) Mitochondria from permeabilized $Bak^{Q75L/Q75L}$ MEFs have a lower threshold for cytochrome *c* release than mitochondria from wild-type cells. An approximately fourfold lower concentration of tBIDM97A induced cytochrome *c* release from pellet (P) containing mitochondria to soluble (S) fractions in $Bak^{Q75L/Q75L}$ compared with $Bak^{+/+}$ MEFs. (*C*) Mitochondria from $Bak^{Q75L/Q75L}$ MEFs require a higher (approximately fourfold) concentration of full-length BCL-X_L to inhibit cytochrome *c* release in response to tBIDM97A (9 nM) treatment. (*D–G*) MEFs were treated with bortezomib (proteasome inhibitor) (*D*), actinomycin D (transcription inhibitor) (*E*), etoposide (topoisomerase inhibitor) (*F*), or cycloheximide (translation inhibitor) (*G*) for 24 h prior to measurement of cell viability by FACS following propidium iodide staining. The percent viability is the PI^{-ve} population in treated cells relative to the same population in cells treated with vehicle (DMSO). Data in *A* and *D–F* are presented as mean ± SD of $n = 3–4$ experiments.

mice is a T-cell-intrinsic defect, consistent with reduced restraint of Bak by Bcl-x_L.

Mode 2 regulates the homeostatic turnover of platelets in vivo

It is well documented that Bcl-2 prosurvival proteins govern platelet survival. The critical regulator of viability in these cells is Bcl-x_L. Genetic deletion or pharmacological inhibition of Bcl-x_L causes severe thrombocytopenia due to reduced platelet life span or induction of apoptosis, respectively (Mason et al. 2007; Zhang et al. 2007; Kodama et al. 2010; Wilson et al. 2010). The main effector of platelet apoptosis is Bak, as deletion of *Bak* causes thrombocythemia (an increase in platelet count) due to an almost doubling of circulating platelet life span (Mason et al. 2007; Josefsson et al. 2011). If mode 2 were operative in platelets, our data suggested that any reduction in the capacity of Bcl-x_L to physically restrain Bak would lead to premature platelet cell death. In agreement with this prediction, $Bak^{+/Q75L}$ and $Bak^{Q75L/Q75L}$ mice displayed platelet counts fivefold to 10-fold lower than wild-type counterparts (Fig. 5A). Platelet life span was dramatically decreased, with $t_{1/2}$ reduced from ~5 d in wild-type animals to <5 h in $Bak^{+/Q75L}$ littermates and ~2.5 h in $Bak^{Q75L/Q75L}$ (Fig. 5B). Consistent with the changes in platelet survival being responsible for the thrombocytopenia, no reduction in megakaryocytes (platelet cell precursors) was observed in the mutants. Indeed, mature megakaryocyte numbers were elevated in $Bak^{+/Q75L}$ and $Bak^{Q75L/Q75L}$ mice (Fig. 5C), presumably a response to thrombocytopenia.

We next examined the role of Bax. Loss of one *Bax* allele had no impact on the thrombocytopenia in $Bak^{+/Q75L}$ mice; however, platelet numbers increased significantly when Bax was fully deleted (Fig. 5D). Bax deletion had no effect in $Bak^{+/+}$ mice, as previously reported (Mason et al. 2007). This indicates that Bax contributes to platelet cell death when Bak is not inhibited by Bcl-x_L. In contrast, deletion of Bim, a BH3-only protein that can both functionally neutralize Bcl-x_L and directly activate Bax and Bak, had no effect on platelet numbers in $Bak^{+/Q75L}$ animals (Fig. 5E), although $Bim^{-/-}$ mice had reduced platelets compared with wild-type animals, consistent with previous reports (Bouillet et al. 1999). Hence, Bim is redundant for Bak and Bax activation in platelets and likely does not affect the ability of Bcl-x_L to restrain either effector molecule. Given that Bax contributes to platelet death when Bak is not restrained by Bcl-x_L, these data could suggest that Bak itself is a Bax activator, possibly via a "feed-forward" mechanism, as recently proposed (Chen et al. 2015). We therefore tested whether a Bak^{Q75L} BH3 peptide could activate purified recombinant BAX and found that it efficiently converted BAX to a dimer (Supplemental Fig. S2). Hence, in platelets, Bax can potentially be activated by unrestrained, activated Bak.

Discussion

Genetic studies have proven invaluable in establishing which of the Bcl-2 family members regulate the life and death of various tissues and cell types (Youle and Strasser 2008); however, they have not provided unambiguous

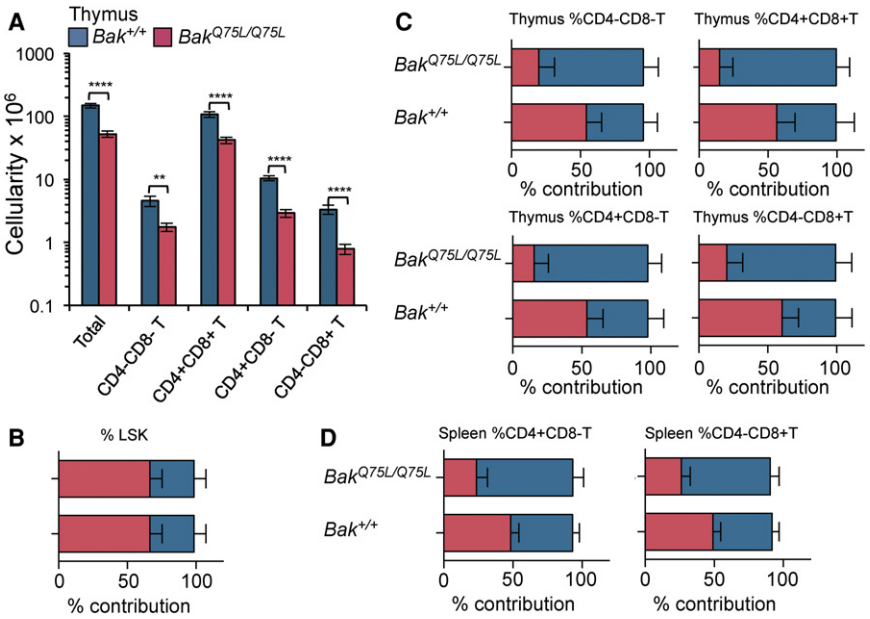

Figure 4. Loss of Bak restraint by Bcl-x_L causes reduced T-cell survival in vivo. (*A*) Thymus cellularity is reduced by approximately threefold in $Bak^{Q75L/Q75L}$ mice ($n = 15$) compared with $Bak^{+/+}$ mice ($n = 11$). (*B*) Thymocyte defects were not due to defects in lineage-negative (Lin^-)/stem cell antigen 1-positive ($Sca1^+$)/Kit^+ (LSK) progenitor cells, as these were not affected by the Q75L mutation. (*C*) $Bak^{Q75L/Q75L}$ thymic T cells were underrepresented compared with $Bak^{+/+}$ T cells in competitive bone marrow transplantation experiments. $n = 6$. (*D*) The representation of $Bak^{Q75L/Q75L}$ cells in splenic $CD44^{low}$ $CD62L^+$ naïve T cells was similar to that of the thymic compartment. Data are presented as mean ± SEM. (****) $P < 0.0001$; (**) $P < 0.01$, Student's unpaired *t*-test.

insight into the mechanisms underlying apoptosis regulation in vivo. Such ambiguities arise because most genetic manipulations disrupt both mode 1 and mode 2 cell death regulation. Deleting a prosurvival protein prevents it from sequestering BH3-only proteins (mode 1) and inhibiting Bak and/or Bax (mode 2). A similar scenario arises with knockout studies involving BH3-only family members. For example, recent data from *Bim*/*Bid*/*Puma*/*Noxa* quadruple-knockout mice provided evidence that activator BH3-only proteins (mode 1) are required for developmental cell death (e.g., removal of interdigital webbing). However, these BH3-only proteins also antagonize mode 2

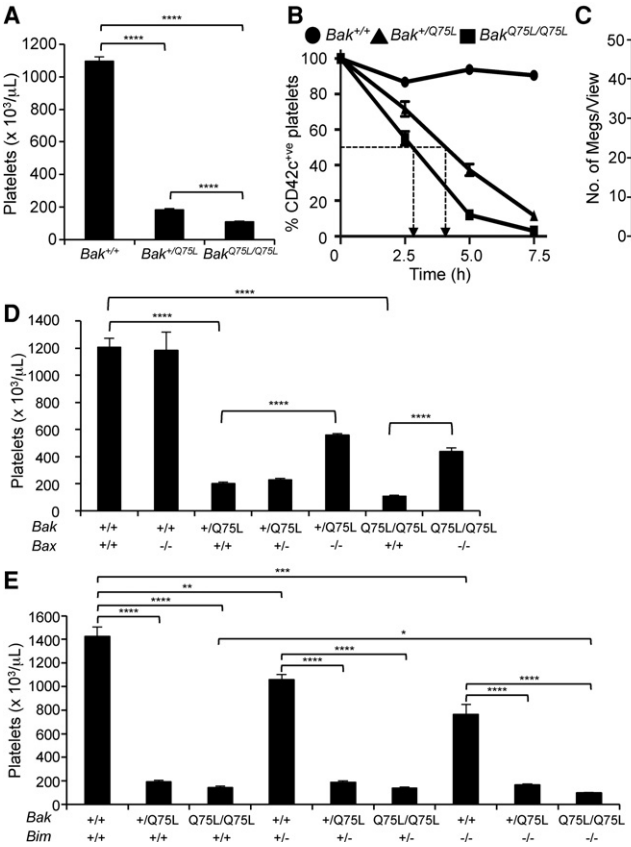

Figure 5. Bcl-x_L restrains Bak to inhibit platelet death. (*A*) $Bak^{+/Q75L}$ and $Bak^{Q75L/Q75L}$ mice had significantly decreased platelet numbers compared with $Bak^{+/+}$ mice. $n = 20$. (*B*) Platelets harboring the Q75L mutation have a reduced life span. $n = 8$ for $Bak^{Q75L/Q75L}$; $n = 4$ for $Bak^{+/Q75L}$. $t_{1/2}$ is indicated by a dotted line. Platelets from wild-type mice have a $t_{1/2}$ of ~5 d. $n = 4$. (*C*) The effect of the Q75L mutation on platelet numbers is not due to impaired megakaryopoiesis, as the number of mature megakaryocytes was elevated in both $Bak^{+/Q75L}$ and $Bak^{Q75L/Q75L}$ mice compared with wild-type mice. $n = 12$. (*D*) Loss of Bax resulted in increased platelet counts in $Bak^{+/Q75L}$ and $Bak^{Q75L/Q75L}$ mice. $n = 3$–8. (*E*) Loss of Bim has no effect on platelet levels in platelets harboring the Q75L mutation ($n = 4$–17), although loss of Bim alone resulted in thrombocytopaenenia, as previously observed. Data are presented as mean ± SEM. (****) $P < 0.0001$; (**) $P < 0.01$; (*) $P < 0.05$, Student's unpaired *t*-test.

interactions; hence, it remains unclear whether one or both of these mechanisms is at play.

The identification of the Bak^{Q75L} mutation allowed us to clarify this situation, as it disrupts a mode 2 interaction (specifically, the physical restraint of Bak by Bcl-x_L) without impairing either mode 1 interactions or Bak's killing activity. Indeed, the Bak^{Q75L} mouse essentially acts as an in vivo reporter of cellular dependence on the Bak:Bcl-x_L interaction. Even at steady state, it is clear that primary cells in vivo rely on the physical restraint of Bak by Bcl-x_L to survive. Specifically, mode 2 regulation is critical for T-cell development, although previous in vitro studies have shown a role for mode 1, with Bcl-x_L inhibiting T-cell apoptosis via engagement of Bim (Liu et al. 2006). Mode 2 is also critical for platelet life span. Platelets circulate in the bloodstream until they encounter one of two fates: consumption by hemostatic processes (i.e., blood clotting) or apoptotic clearance. The latter is mediated by Bak (Mason et al. 2007). In Bak^{Q75L} mice, our data indicate that Bcl-x_L is unable to restrain Bak for the normal duration of platelet circulation. Premature entry into apoptosis shortens platelet life span, leading to thrombocytopenia. The partial rescue of platelet counts in Bak^{Q75L} mice following *Bax* deletion demonstrates that Bax contributes to platelet death once Bcl-x_L and Bak become disengaged. Whether this is via a feed-forward activation mechanism (similar to that proposed based on in vitro studies) (Llambi et al. 2011; Chen et al. 2015; Dai et al. 2015) will require further investigation.

Despite their hematopoietic defects, $Bak^{+/Q75L}$ and $Bak^{Q75L/Q75L}$ mice appear outwardly healthy to at least 6 mo of age. This supports the view that the Q75L mutation influences only interaction with Bcl-x_L and not other prosurvival proteins, as the mutant mouse phenotype would be more severe, as seen in Mcl-1-deficient (or Bcl-2-deficient) mice. For example, mature B-cell numbers do not change significantly in $Bak^{Q75L/Q75L}$ mice (Supplemental Fig. S3), although these are profoundly affected by Mcl-1 or Bcl-2 deficiency. Hence, restraint of Bak by other prosurvival proteins is sufficient to prevent Bak-mediated apoptosis in most tissues. The most likely candidate is Mcl-1, which, like Bcl-x_L, engages Bak BH3 with high affinity and is widely expressed. Our MEF data provide strong support of this proposition, as Bak^{Q75L} cells more readily succumb to apoptotic triggers that have an impact on Mcl-1 functionality (e.g., Noxa induction via etoposide and bortezomib) or levels (e.g., cycloheximide treatment).

Our in vitro studies demonstrate a direct (inverse) correlation between Bak:Bcl-x_L affinity and a drug's killing activity, demonstrating that the strength of the mode 2 interaction sets the threshold for drug-induced apoptosis. This is consistent with recent reports showing that activated BAK levels (or BAK:prosurvival protein complexes) dictate chemosensitivity (Dai et al. 2015) and that mode 2 is more efficient than mode 1 at inhibiting apoptosis (Llambi et al. 2011). Although previous studies implicated prosurvival protein "priming" by BH3-only proteins as a key determinant of drug sensitivity (Certo et al. 2006; Vo et al. 2012), these new data argue that the strength of mode 2 interactions (which varies widely for prosurvival:Bax/Bak protein pairs) is also important.

In summary, the Bak^{Q75L} mice provide the first in vivo evidence of the physiological importance of mode 2 regulation and broader insights into how prosurvival proteins control cell fate.

Materials and methods

Recombinant proteins

Recombinant human and mouse Bcl-2 prosurvival proteins with N-terminal and/or C-terminal truncations for binding studies (h/mBCL-2ΔC22, h/mBCL-X_LΔC24, mBcl-x_LY101FΔC24, mBcl-x_LQ111AΔC24, mBcl-x_LY101F/Q111AΔC24, h/mBCL-W C29S/A128EΔC29, h/mMCL-1ΔN170ΔC23, and h/mBFL-1ΔC19); the loop-deleted form of hBCL-X_L (ΔN27–82ΔC24) and hBAKΔN22ΔC25Q77L used for crystallization; and full-length hBCL-X_L, htBID, hBAXΔC21, and htBIDM97A used in other studies were all expressed and purified exactly as described previously (Kluck et al. 1999; Chen et al. 2005; Moldoveanu et al. 2006; Lee et al. 2007, 2008; Czabotar et al. 2013; Hockings et al. 2015).

Synthetic peptides

Synthetic peptides were synthesized by Mimotopes and purified by reverse-phase high-performance liquid chromatography (HPLC) to ≥90% purity. The peptides used in this study were hBAK BH3 (LPLQPSSTMGQVGRQLAIIGDDINRRYDSEFQTM), mBak BH3 (LPLEPNSILGQVGRQLALIGDDINRRYDTEFQNL), mBak Q75L BH3 (LPLEPNSILGQVGRLLALIGDDINRRYDTEFQNL), BIM BH3 (DMRPEIWIAQELRRIGDEFNAYYARR), BAD BH3 (NLWAAQRYGRELRRMSDEFVDSFKKG), and BID M97A BH3 (SQEDIIRNIARHLAQVGDSADRSIPPG).

Phage display binding studies

A 26-amino-acid residue peptide encompassing the Flag-tagged BAK BH3 domain plus flanking residues (PSSTMGQVGRQLAIIGDDINRRYDSE) was fused via a linker sequence (GGGT) to the N terminus of the M13 phage *gene3* in the phagemid vector described previously (Fairlie et al. 2003). Alanine-scanning constructs and phage particles were isolated from cell supernatants and tested in phage competition ELISAs as described previously (Lee et al. 2008).

Surface plasmon resonance competitive binding assays

Solution competition assays were performed by using a Biacore 3000 instrument (GE Healthcare) as described previously (Lee et al. 2009). In brief, recombinant, 10 nM purified human or mouse prosurvival proteins was incubated with varying concentrations of peptide for at least 2 h in running buffer (10 mM HEPES at pH 7.4, 150 mM NaCl, 3.4 mM EDTA, 0.005% [v/v] Tween20) prior to injection onto a CM5 sensor chip on which either wild-type BIM BH3 or an inert BIM BH3 mutant peptide (BIM4E) was immobilized. Specific binding of the prosurvival protein to the surface in the presence and absence of competitor peptides was quantified by subtracting the signal obtained on the BIM mutant channel from that obtained on the wild-type BIM channel.

Cell lines

The *Bak*$^{+/+}$, *Bak*$^{+/Q75L}$, and *Bak*$^{Q75L/Q75L}$ MEFs were generated from embryonic day 13.5–14 embryos and immortalized (at passage 2–4) with SV40 large T antigen. To generate cell lines expressing BAK mutants, MEFs were transduced with retroviruses in which expression of each protein was linked to GFP expression or a hygromycin resistance gene via an internal ribosome entry site sequence in pMIG or pMIH vectors. Following infection, GFP^{+ve} cells (generated from pMIG retroviruses) were sorted, while cells infected with pMIH retroviruses were selected by growing them in 250 μg/mL hygromycin. Cells were maintained in DME KELSO medium supplemented with 10% (v/v) fetal bovine serum, 250 μM L-asparagine, and 50 μM 2-mercaptoethanol.

Cell-killing assays

For long-term clonogenic survival assays, MEFs were transduced with the indicated constructs in which expression of each protein was linked to GFP or mCherry expression via an internal ribosome entry site sequence. GFP^{+ve} or GFP^{+ve} plus mCherry^{+ve} cells (in cases where the effect of gene coexpression was examined) were then sorted and plated at 150 cells per well in six-well plates and incubated for 7 d. Colonies were then stained with Coomassie blue and counted. Short-term killing assays were performed on cells treated with various drugs (etoposide, bortezomib, actinomycin D, and cycloheximide). Twenty-four hours after treatment, cells were stained with 5 μg/mL propidium idodide and then analyzed by FACS (FACSCalibur, BD Biosciences). Cell viability was determined by establishing the fraction of PI^{-ve} cells relative to the same population in cells treated with vehicle (DMSO) alone.

Mutagenesis screen and isolation of the Bak^{Q75L} mutation

Male BALB/c mice were injected intraperitoneally with 85 mg/kg ENU (Sigma-Aldrich) weekly for 3 wk. Twelve weeks after the last cycle, mice were mated with untreated BALB/c females to produce first-generation (G_1) progeny. Peripheral blood from these animals was taken at 7 wk of age, and blood cell counts were analyzed using an ADVIA 2120 hematology analyzer (Siemens). Mice with low platelet counts were rebled at 9 wk of age to confirm a stable phenotype and then crossed to C57BL/6. Thrombocytopenic F_1 offspring were back-crossed to C57BL/6 to generate F_1N_1 offspring. Twenty-one affected F_1N_1 mice were genotyped for 660 SNPs spaced at 5- to 10-Mb intervals throughout the genome using the iPLEX Gold method, the MassARRAY system (Sequenom), and an Autoflex MALDI-TOF mass spectrometer (Bruker) at the Australian Genome Research Facility (AGRF). Haplotypes were constructed, and regions of heterozygosity were identified using Excel version 14.3.4 software (Microsoft). Additional F_1N_1 mice were genotyped for more finely spaced SNPs using the Amplifluor SNP HT genotyping system FAM-JOE (Merck Millipore). Results were visualized, and genotypes were assigned using assayauditorEP.xls (Merck Millipore) and Excel version 14.3.4 software (Microsoft). The causative lesion was mapped to a 4.5-Mb region between rs13482920 and rs13482937 on chromosome 17. Candidate genes were sequenced by Sanger sequencing at the AGRF. Experimental mice were backcrossed onto C57BL/6 background for >10 generations prior to crossing onto *Bax*$^{-/-}$ and *Bim*$^{-/-}$ strains. All animal experiments complied with the regulatory standards of and were approved by the Walter and Eliza Hall Institute Animal Ethics Committee.

In vivo assessment of platelet life span

Mice were injected intravenously with the fluorescently labeled rat anti-GPIbβ X488 antibody (Emfret) at 0.15 μg per gram of body weight. Platelet life span was measured by flow cytometry as previously described (Josefsson et al. 2012). Mice were bled from the tail vein every 2.5 h, and platelets were identified in platelet-rich plasma as being CD41$^+$, with the proportion of X488$^+$ remaining cells assessed at each time point.

Competitive bone marrow transfer experiments

Mixed bone marrow chimeras were generated by transplanting a 1:3 ratio of Ly5.1$^+$ competitor cells and Ly5.2$^+$ test cells (5×10^6 total bone marrow cells) into lethally irradiated (1100 rad) Ly5.1$^+$ Ly5.2$^+$ recipients. Test bone marrow cells were isolated from wild-type, *Bak*$^{+/Q75L}$, or *Bak*$^{Q75L/Q75L}$ mice. Bone marrow chimeras were analyzed 12 wk after reconstitution by flow cytometry performed with a Fortessa (BD Biosciences), and data were analyzed using FlowJo software (Tree Star). Monoclonal antibodies were produced at the Walter and Eliza Hall Institute unless otherwise indicated and labeled in-house with fluorescein isothiocyanate, R-phycoerythrin, R-phycoerythrin-Cy7, allophycocyanin, Alexa700, or biotin. Clone numbers were CD4 (GK1.5), CD8 (53.6.7), CD19 (1D3), CD44 (IM7), CD45.1 (A20), CD45.2 (S450-15-2), TER119 (Ly76), GR1 (RB6-8C5), CD11b (M1/70), Sca1 (D7), Kit (ACK4), and B220 (RA3-6B2). CD62L-allophycocyanin was purchased from eBioscience. Streptavidin PE-Texas red was purchased from Life Technologies. Fluoro-Gold (Sigma) was used to exclude dead cells.

Hemopoietic analysis

Single-cell suspensions were prepared from the spleen and thymus, and viable leukocytes from 60 d-old mice were determined with a CASY cell counter (Scharfe System GmbH). Blood cell counts were determined using an ADVIA 2120 hematology analyzer (Siemens) and then depleted of red cells by treatment with 0.168 M ammonium chloride before FACS analysis. The composition of leukocyte populations was determined by flow cytometric analysis on a FASCalibur (BD Biosciences) following staining with fluorochrome-labeled surface marker-specific monoclonal antibodies, and data were analyzed using FlowJo version 9.3.2 (TreeStar). The monoclonal antibodies were produced and labeled with fluorescein isothiocyanate, R-phycoerythrin, or allophycocyanin at the Walter and Eliza Hall Institute unless otherwise indicated. Antibody clone numbers were CD4 (YTA3.2.1), CD8 (YTS169), THY-1 (T24.3.21), IgM (5.1), IgD (11-26C), B220 (RA3-6B2), c-Kit (ACK-4), GR-1 (RB6-8C5), MAC-1 (MI/70), CD3 (145-2C11), and B220 (RA3-6B2).

Cytochrome c *release assay*

MEFs were permeabilized in digitonin containing buffer (20 mM HEPES at pH 7.2, 100 mM KCl, 5 mM $MgCl_2$, 1 mM EDTA, 1 mM EGTA, 1250 mM sucrose, 0.05% [w/v] digitonin) and incubated with tBIDM97A for 1 h at 30°C before pelleting via centrifugation. The supernatant was retained (soluble fraction), and the pellet was lysed in Triton X-100-containing buffer (20 mM Tris at pH 7.4, 135 mM NaCl, 1.5 mM $MgCl_2$, 1 mM EDTA, 10% [v/v] glycerol, 1% [v/v] Triton X-100, protease inhibitors) to generate the pellet fraction. In experiments examining BCL-X_L inhibition of cytochrome *c* release, various concentrations of recombinant full-length hBCL-X_L were added immediately prior to the addition of 9 nM tBIDM97A. Both soluble and pellet fractions were

analyzed for cytochrome *c* by Western blotting using an anti-cytochrome *c* antibody (BD Biosciences, clone 7H8.2C12).

Blue Native PAGE of BAK oligomerization

Membrane fractions from MEFs (wild-type, $Bak^{+/Q75L}$, $Bak^{Q75L/Q75L}$, or $Bax^{-/-}/Bak^{-/-}$ reconstituted with BAK mutants) were generated by permeabilizing cells with 0.025% (w/v) digitonin in permeabilization buffer (20 mM HEPES/KOH at pH 7.5, 100 mM sucrose, 2.5 mM $MgCl_2$, 50 mM KCl supplemented with Complete protease inhibitors [Roche], 2 mM DTT). Membrane fractions were then treated for 30 min at 30°C in the presence or absence of recombinant tBID prior to solubilization in 20 mM Bis-tris (pH 7.4), 50 mM NaCl, 10% (v/v) glycerol, 2 mM DTT, and 1% (w/v) digitonin. Insoluble debris was removed by centrifugation at 13,000*g*, and 10× BN-PAGE loading dye (5% [w/v] Coomassie blue G-250 [Bio-Rad] in 500 mM 6-aminohexanoic acid, 100 mM Bis-tris at pH 7.0) was then added. Samples were electrophoresed on 4%–13% native gels in anode buffer (50 mM Bis-tris at pH 7.0) and blue cathode buffer (50 mM Tricine, 15 mM Bis-tris unbuffered containing 0.02% [w/v] Coomassie blue G-250), with blue cathode buffer replaced with clear buffer (without Coomassie blue) when the dye front was one-third through the resolving gel. Gels were transferred to PVDF and immunoblotted for BAK (7D10).

Immunoprecipitation assays

MLM were prepared as described (Uren et al. 2005). MLM were diluted to 1 mg/mL in MELB (100 mM KCl, 2.5 mM $MgCl_2$, 100 mM sucrose, 20 mM HEPES/KOH at pH 7.5, 5 mM DTT) supplemented with protease inhibitor cocktail, 4 mg/mL pepstatin A, and 5 mM DTT. Full-length human BCL-X_L or mouse Mcl-1ΔN170ΔC23 (both at 32 nM) was preincubated with MLM for 20 min at 37°C before addition of 30 nM tBIDM97A as indicated and incubation for a further 2 h at 37°C. Samples were solubilized with 1% (w/v) digitonin and immunoprecipitated as described (Dewson et al. 2008) using anti-BCL-X_L IC2 rat (Willis et al. 2005) or anti-Mcl-1 14C11 rat (Banerjee et al. 2008) monoclonal antibodies.

Protein crystallization

The BAK BH3:BCL-X_L and BakQ75L BH3:BCL-X_L peptide complexes used a "loop-deleted" form of human BCL-X_L (Δ27–82 and, without membrane anchor, residues 210–233), which forms an α1 domain-swapped dimer yet retains BH3 domain-binding activity (Lee et al. 2007). Crystals were obtained by mixing BCL-X_L with the BH3 peptides at a molar ratio of 1:1.3 and then concentrating the sample to 10 mg/mL. Crystallization trials were performed at the Bio21 Collaborative Crystallisation Centre. BAK BH3:BCL-X_L complex crystals were grown by the sitting drop method at room temperature in 0.16 M calcium acetate, 0.08 M sodium cacodylate (pH 6.5), 20% (v/v) glycerol, 14.4% (w/v) PEG 8000, and, for the BCL-X_L:BakQ75L BH3 complex, in 0.2 M sodium thiocyanate and 20% (w/v) PEG 3350. BAKΔN22ΔC25Q77L crystals were grown in 10% (w/v) PEG 3350, 0.1 M sodium acetate (pH 4.5), and 20 mM zinc acetate, similar to the conditions previously reported for wild-type BAK (Moldoveanu et al. 2006). Prior to cryocooling in liquid N_2, BakQ75L BH3:BCL-X_L and BAKΔN22ΔC25Q77L crystals were equilibrated into cryoprotectant consisting of reservoir solution containing 15% (v/v) ethylene glycol. Crystals were mounted directly from the drop and plunge-cooled in liquid N_2.

Crystal diffraction data collection and structure determination

Diffraction data were collected at 100 K at the Australian Synchrotron MX1 and MX2 beamlines (wave-length for all structures was 0.95364 Å). The diffraction data were integrated and scaled with either HKL2000 (Otwinowski and Minor 1997) for the BAK BH3:BCL-X_L structure or XDS (Kabsch 2010) for the BAKQ75L BH3:BCL-X_L and full-length BAKQ77L structures. The structures were solved by molecular replacement with Phaser (McCoy et al. 2005) using the previous crystal structures of BCL-X_L from the BECLIN BH3:BCL-X_L complex (Protein Data Bank [PDB] ID 2P1L) (Oberstein et al. 2007) with the BECLIN BH3 peptide removed for the BCL-X_L peptide complex structures or the wild-type BAK (PDB ID 2IMS) for the BAKQ77L structure as search models. Multiple rounds of building in COOT (Emsley and Cowtan 2004) and refinement in PHENIX (Kabsch 2010) led to the final models.

BAX dimerization assay

The dimerization of BAX treated with BH3 peptides was performed as described previously (Czabotar et al. 2013). Briefly, recombinant BAXΔC21 was incubated with threefold molar excess of each peptide in Tris-buffered saline (pH 8.0) containing 1.0% (w/v) CHAPS. Dimerization was assessed by gel filtration chromatography on a Superdex 75 10/300 column.

Acknowledgments

We thank Lorraine O'Reilly (Walter and Eliza Hall Institute) and Andreas Strasser (Walter and Eliza Hall Institute) for provision of some antibodies, and Sweta Iyer (Walter and Eliza Hall Institute) for technical assistance. This work was supported by Program Grants (1016701 and 1016647), Project Grants (1041936 and 575561), a Career Development Fellowship (1024620), and Fellowships (1022618, 1063008, 1042629, and 1079700) from the National Health and Medical Research Council of Australia; a Fellowship (FT100100791) from the Australian Research Council (ARC); a Cancer Council of Victoria Grant-in-Aid (1057949); and a Specialised Center of Research grant (7015) from the Leukemia and Lymphoma Society. S.G. was supported by Cancer Council of Victoria, Leukaemia Foundation Australia, the Lady Tata Memorial Trust, Melbourne International Research, the Melbourne International Fee Remission Scholarship (University of Melbourne), and Cancer Therapeutics CRC Top-up Scholarship. Infrastructure support was provided by National Health and Medical Research Council of Australia Independent Research Institute Infrastructure Support Scheme grant 361646 and a Victorian State Government Operational Infrastructure Program grant.

References

Banerjee A, Grumont R, Gugasyan R, White C, Strasser A, Gerondakis S. 2008. NF-κB1 and c-Rel cooperate to promote the survival of TLR4-activated B cells by neutralizing Bim via distinct mechanisms. *Blood* **112:** 5063–5073.

Bouillet P, Metcalf D, Huang DC, Tarlinton DM, Kay TW, Kontgen F, Adams JM, Strasser A. 1999. Proapoptotic Bcl-2 relative Bim required for certain apoptotic responses, leukocyte homeostasis, and to preclude autoimmunity. *Science* **286:** 1735–1738.

Certo M, Del Gaizo Moore V, Nishino M, Wei G, Korsmeyer S, Armstrong SA, Letai A. 2006. Mitochondria primed by death

signals determine cellular addiction to antiapoptotic BCL-2 family members. *Cancer Cell* **9:** 351–365.

Chen L, Willis SN, Wei A, Smith BJ, Fletcher JI, Hinds MG, Colman PM, Day CL, Adams JM, Huang DC. 2005. Differential targeting of prosurvival Bcl-2 proteins by their BH3-only ligands allows complementary apoptotic function. *Mol Cell* **17:** 393–403.

Chen HC, Kanai M, Inoue-Yamauchi A, Tu HC, Huang Y, Ren D, Kim H, Takeda S, Reyna DE, Chan PM, et al. 2015. An interconnected hierarchical model of cell death regulation by the BCL-2 family. *Nat Cell Biol* **17:** 1270–1281.

Cheng EH, Wei MC, Weiler S, Flavell RA, Mak TW, Lindsten T, Korsmeyer SJ. 2001. BCL-2, BCL-X_L sequester BH3 domain-only molecules preventing BAX- and BAK-mediated mitochondrial apoptosis. *Mol Cell* **8:** 705–711.

Cheng EH, Sheiko TV, Fisher JK, Craigen WJ, Korsmeyer SJ. 2003. VDAC2 inhibits BAK activation and mitochondrial apoptosis. *Science* **301:** 513–517.

Czabotar PE, Westphal D, Dewson G, Ma S, Hockings C, Fairlie WD, Lee EF, Yao S, Robin AY, Smith BJ, et al. 2013. Bax crystal structures reveal how BH3 domains activate Bax and nucleate its oligomerization to induce apoptosis. *Cell* **152:** 519–531.

Dai H, Ding H, Meng XW, Peterson KL, Schneider PA, Karp JE, Kaufmann SH. 2015. Constitutive BAK activation as a determinant of drug sensitivity in malignant lymphohematopoietic cells. *Genes Dev* **29:** 2140–2152.

Dewson G, Kratina T, Sim HW, Puthalakath H, Adams JM, Colman PM, Kluck RM. 2008. To trigger apoptosis, Bak exposes its BH3 domain and homodimerizes via BH3:groove interactions. *Mol Cell* **30:** 369–380.

Emsley P, Cowtan K. 2004. COOT: model-building tools for molecular graphics. *Acta Crystallogr D Biol Crystallogr* **60:** 2126–2132.

Fairlie WD, Uboldi AD, Hemmings GJ, Smith BJ, Martin HM, Morgan PO, Baca M. 2003. A family of leukemia inhibitory factor-binding peptides that can act as antagonists when conjugated to poly(ethylene glycol). *Biochemistry* **42:** 13193–13201.

Fletcher JI, Meusburger S, Hawkins CJ, Riglar DT, Lee EF, Fairlie WD, Huang DC, Adams JM. 2008. Apoptosis is triggered when prosurvival Bcl-2 proteins cannot restrain Bax. *Proc Natl Acad Sci* **105:** 18081–18087.

Hockings C, Anwari K, Ninnis RL, Brouwer J, O'Hely M, Evangelista M, Hinds MG, Czabotar PE, Lee EF, Fairlie WD, et al. 2015. Bid chimeras indicate that most BH3-only proteins can directly activate Bak and Bax, and show no preference for Bak versus Bax. *Cell Death Dis* **6:** e1735.

Josefsson EC, James C, Henley KJ, Debrincat MA, Rogers KL, Dowling MR, White MJ, Kruse EA, Lane RM, Ellis S, et al. 2011. Megakaryocytes possess a functional intrinsic apoptosis pathway that must be restrained to survive and produce platelets. *J Exp Med* **208:** 2017–2031.

Josefsson EC, White MJ, Dowling MR, Kile BT. 2012. Platelet life span and apoptosis. *Methods Mol Biol* **788:** 59–71.

Kabsch W. 2010. Xds. *Acta Crystallogr D Biol Crystallogr* **66:** 125–132.

Kluck RM, Esposti MD, Perkins G, Renken C, Kuwana T, Bossy-Wetzel E, Goldberg M, Allen T, Barber MJ, Green DR, et al. 1999. The pro-apoptotic proteins, Bid and Bax, cause a limited permeabilization of the mitochondrial outer membrane that is enhanced by cytosol. *J Cell Biol* **147:** 809–822.

Kodama T, Takehara T, Hikita H, Shimizu S, Li W, Miyagi T, Hosui A, Tatsumi T, Ishida H, Tadokoro S, et al. 2010. Thrombocytopenia exacerbates cholestasis-induced liver fibrosis in mice. *Gastroenterology* **138:** 2487–2498.

Kuwana T, Bouchier-Hayes L, Chipuk JE, Bonzon C, Sullivan BA, Green DR, Newmeyer DD. 2005. BH3 domains of BH3-only proteins differentially regulate Bax-mediated mitochondrial membrane permeabilization both directly and indirectly. *Mol Cell* **17:** 525–535.

Lazarou M, Stojanovski D, Frazier AE, Kotevski A, Dewson G, Craigen WJ, Kluck RM, Vaux DL, Ryan MT. 2010. Inhibition of Bak activation by VDAC2 is dependent on the Bak transmembrane anchor. *J Biol Chem* **285:** 36876–36883.

Leber B, Lin J, Andrews DW. 2010. Still embedded together binding to membranes regulates Bcl-2 protein interactions. *Oncogene* **29:** 5221–5230.

Lee EF, Czabotar PE, Smith BJ, Deshayes K, Zobel K, Colman PM, Fairlie WD. 2007. Crystal structure of ABT-737 complexed with Bcl-x_L: implications for selectivity of antagonists of the Bcl-2 family. *Cell Death Differ* **14:** 1711–1713.

Lee EF, Czabotar PE, van Delft MF, Michalak EM, Boyle MJ, Willis SN, Puthalakath H, Bouillet P, Colman PM, Huang DC, et al. 2008. A novel BH3 ligand that selectively targets Mcl-1 reveals that apoptosis can proceed without Mcl-1 degradation. *J Cell Biol* **180:** 341–355.

Lee EF, Sadowsky JD, Smith BJ, Czabotar PE, Peterson-Kaufman KJ, Colman PM, Gellman SH, Fairlie WD. 2009. High-resolution structural characterization of a helical α/β-peptide foldamer bound to the anti-apoptotic protein Bcl-xL. *Angew Chem Int Ed Engl* **48:** 4318–4322.

Letai A, Bassik MC, Walensky LD, Sorcinelli MD, Weiler S, Korsmeyer SJ. 2002. Distinct BH3 domains either sensitize or activate mitochondrial apoptosis, serving as prototype cancer therapeutics. *Cancer Cell* **2:** 183–192.

Liu X, Zhu Y, Dai S, White J, Peyerl F, Kappler JW, Marrack P. 2006. Bcl-xl does not have to bind Bax to protect T cells from death. *J Exp Med* **203:** 2953–2961.

Llambi F, Moldoveanu T, Tait SW, Bouchier-Hayes L, Temirov J, McCormick LL, Dillon CP, Green DR. 2011. A unified model of mammalian BCL-2 protein family interactions at the mitochondria. *Mol Cell* **44:** 517–531.

Ma A, Pena JC, Chang B, Margosian E, Davidson L, Alt FW, Thompson CB. 1995. Bclx regulates the survival of double-positive thymocytes. *Proc Natl Acad Sci* **92:** 4763–4767.

Mason KD, Carpinelli MR, Fletcher JI, Collinge JE, Hilton AA, Ellis S, Kelly PN, Ekert PG, Metcalf D, Roberts AW, et al. 2007. Programmed anuclear cell death delimits platelet life span. *Cell* **128:** 1173–1186.

McCoy AJ, Grosse-Kunstleve RW, Storoni LC, Read RJ. 2005. Likelihood-enhanced fast translation functions. *Acta Crystallogr D Biol Crystallogr* **61:** 458–464.

Merino D, Giam M, Hughes PD, Siggs OM, Heger K, O'Reilly LA, Adams JM, Strasser A, Lee EF, Fairlie WD, et al. 2009. The role of BH3-only protein Bim extends beyond inhibiting Bcl-2-like prosurvival proteins. *J Cell Biol* **186:** 355–362.

Moldoveanu T, Liu Q, Tocilj A, Watson M, Shore G, Gehring K. 2006. The X-ray structure of a BAK homodimer reveals an inhibitory zinc binding site. *Mol Cell* **24:** 677–688.

Motoyama N, Wang F, Roth KA, Sawa H, Nakayama K, Nakayama K, Negishi I, Senju S, Zhang Q, Fujii S, et al. 1995. Massive cell death of immature hematopoietic cells and neurons in Bcl-x-deficient mice. *Science* **267:** 1506–1510.

Oberstein A, Jeffrey PD, Shi Y. 2007. Crystal structure of the Bcl-XL–Beclin 1 peptide complex: Beclin 1 is a novel BH3-only protein. *J Biol Chem* **282:** 13123–13132.

Otwinowski Z, Minor W. 1997. Processing of X-ray diffraction data collected in oscillation mode. *Methods Enzymol* **276:** 307–326.

Uren RT, Dewson G, Bonzon C, Lithgow T, Newmeyer DD, Kluck RM. 2005. Mitochondrial release of pro-apoptotic proteins: electrostatic interactions can hold cytochrome c but not Smac/DIABLO to mitochondrial membranes. *J Biol Chem* **280:** 2266–2274.

Vo TT, Ryan J, Carrasco R, Neuberg D, Rossi DJ, Stone RM, Deangelo DJ, Frattini MG, Letai A. 2012. Relative mitochondrial priming of myeloblasts and normal HSCs determines chemotherapeutic success in AML. *Cell* **151:** 344–355.

Willis SN, Chen L, Dewson G, Wei A, Naik E, Fletcher JI, Adams JM, Huang DC. 2005. Proapoptotic Bak is sequestered by Mcl-1 and Bcl-xL, but not Bcl-2, until displaced by BH3-only proteins. *Genes Dev* **19:** 1294–1305.

Willis SN, Fletcher JI, Kaufmann T, van Delft MF, Chen L, Czabotar PE, Ierino H, Lee EF, Fairlie WD, Bouillet P, et al. 2007. Apoptosis initiated when BH3 ligands engage multiple Bcl-2 homologs, not Bax or Bak. *Science* **315:** 856–859.

Wilson WH, O'Connor OA, Czuczman MS, LaCasce AS, Gerecitano JF, Leonard JP, Tulpule A, Dunleavy K, Xiong H, Chiu YL, et al. 2010. Navitoclax, a targeted high-affinity inhibitor of BCL-2, in lymphoid malignancies: a phase 1 dose-escalation study of safety, pharmacokinetics, pharmacodynamics, and antitumour activity. *Lancet Oncol* **11:** 1149–1159.

Youle RJ, Strasser A. 2008. The BCL-2 protein family: opposing activities that mediate cell death. *Nat Rev Mol Cell Biol* **9:** 47–59.

Zhang H, Nimmer PM, Tahir SK, Chen J, Fryer RM, Hahn KR, Iciek LA, Morgan SJ, Nasarre MC, Nelson R, et al. 2007. Bcl-2 family proteins are essential for platelet survival. *Cell Death Differ* **14:** 943–951.

Physiological restraint of Bak by Bcl-x_L is essential for cell survival

Erinna F. Lee, Stephanie Grabow, Stephane Chappaz, et al.

Genes Dev. 2016, **30:** originally published online May 19, 2016
Access the most recent version at doi:10.1101/gad.279414.116